Planar fluorescence sensors for two-dimensional measurements of H_2S distributions and dynamics in sedimentary deposits

Qingzhi Zhu* and Robert C. Aller

School of Marine and Atmospheric Sciences, Stony Brook University, Stony Brook, NY 11794-5000, USA

* Corresponding author. Tel: +1-631-632-8747; fax: +1-631-632-3066.

Email address: qing.zhu@stonybrook.edu (Qingzhi Zhu).

Abstract

Planar fluorescence sensors have been developed for measuring two-dimensional hydrogen sulfide (H_2S) distributions in marine sediments by using pyronin Y (PY) as a novel H_2S indicator. Sensing foils were prepared by non-covalently immobilizing PY in ethyl cellulose polymer membranes on transparent polyester sheets, and coating them with gas permeable silicone. Fluorescence from the sensors emitted at 567 nm (excitation at 554 nm) is inversely correlated to H_2S concentration in solution. Two primary sensor modifications, M1 and M2, were used. The M1 sensor shows an excellent linear response versus H_2S in the range of non-detectable (nd) to 3150 μmol/L with a detection limit of 40 μmol/L H_2S (3σ), and it can be utilized for high concentration H_2S measurement. The M2 sensor has a dynamic working dynamic range of nd – 125 μmol/L H_2S with a detection limit of 4 μmol/L (3σ) and can be used to detect low level H_2S in samples. The response time (t_{90}) and recovery time (R_{90}) of the M1 sensor are ~60 and 30 s, respectively, and for the M2, ~15 s. These fluorosensors are only sensitive to H_2S rather than ionic sulfide and bisulfide species, and their performance is independent of temperature and other dissolved gases such as oxygen, CO_2, NH_3 and N_2. No interferences from major ions and trace elements in sediment porewater were observed due to the protection of the fluorophore by the silicone membrane.

The sensors are simple, stable, and semi-reversible (reversible for M2) for extended periods, and have been successfully used to measure 2-dimensional H_2S distributions and dynamics in sulfidic salt marsh sediments with a theoretical pixel resolution of ~ 50×50 μm. Complex heterogeneous H_2S distributions in marine sediments and previously undocumented time-dependent biogeochemical reaction dynamics associated with both inhabited and abandoned biogenic structures were readily revealed.

Keywords: Hydrogen sulfide planar fluorosensor; pyronin Y; 2-dimensional H_2S distributions in marine sediments.

1. Introduction

Hydrogen sulfide is a highly reactive and biologically toxic solute in marine sediments which is produced primarily from bacterially-mediated sulfate reduction. As a diprotic acid, it may speciate as H_2S, HS^- and S^{2-} and is often measured as total H_2S (ΣH_2S). H_2S has a conditional $pK_1' = 6.5 – 6.6$ and $pK_2' > 13.6$ in seawater, and therefore speciates predominantly as HS^- and H_2S over the pH range of most natural solutions (Goldhaber and Kaplan, 1975; Morse et al., 1987; Millero et al, 1988). Its distribution patterns are directly coupled to multiple biogenic and abiogenic reactions such as sulfide oxidation, sulfate reduction, metal-sulfide precipitation and dissolution, nucleophilic additions to organic matter, and acid-base equilibria (Jørgensen and Kasten, 2006; Berner, 1984; Aller et al., 2010; Morse et al., 1987; Luther et al., 1986, 2011; Schippers and Jørgensen, 2002; Brüchert et al., 2003; Johnston, 2011). Understanding the diagenetic behavior and detailed distribution patterns of H_2S in marine sediments is therefore necessary for studying the pathways of sulfur cycling and the interactions of the sulfur cycle directly or indirectly with other biogeochemical processes (Jørgensen and Kasten, 2006; Canfield, 2004). Because H_2S can be rapidly oxidized by oxygen, nitrate, or iron/manganese oxyhydroxides or precipitated as solid phase sulfides, sharp and dynamic gradients of dissolved H_2S in porewater can be generated along geometrically complex oxic-anoxic interfaces in organic-rich sediments underlying oxygenated seawaters (Morse et al., 1987; Canfield et al., 1992; Brendel and Luther, 1995; Kühl et al., 1998; Brüchert et al., 2003). The

measurement of real-time H_2S distributions in heterogeneous sediments with high spatial and temporal resolution is therefore a significant challenge of major biogeochemical importance.

There have been many different approaches for the determination of hydrogen sulfide including: spectrophotometric (Cline, 1969; Kuban et al., 1992; Mousavi and Sarlack, 1997), fluorescence (Choi and Hawkins, 2003), spectroscopic (Johnson and Coletti, 2002), electrochemical (Luther et al., 1985; Ciglenecki and Cosovic, 1996) and chromatographic methods (Tang and Santschi, 2000). Spectrophotometric methods are the most common approach for sulfide detection in environmental samples (Lawrence et al., 2000). These methods involve reduction of a chromogen with sulfide in the presence of a trace metal catalyst, and utilization of differences in color between the oxidized and reduced chromogen forms. Methylene blue, thionine, crystal violet, resazurin, and toluidine blue have been used as chromogens in this approach (Lawrence et al., 2000), and sulfide selective optical sensors have also been developed using methylene blue and thionine as sulfide indicators (Kohls et al., 1996; Shamsipur et al., 2005). However, these optical sensors are not very suitable for in-situ H_2S measurements due to the irreversible reduction reaction with sulfide, long response times, the need for regeneration of sensor chemistry, and the requirement of a catalyst (Kohls et al., 1996).

Fine scale measurements of vertical H_2S profiles in stratified sediments and biofilms have been performed by various H_2S electrochemical microsensors at submillimeter scale resolution (Berner, 1963; Brendel and Luther, 1995; Ciglenecki and Cosovic, 1996; Kühl et al., 1998; Luther et al., 1998, 1999; Revsbech, 2005). The sharp H_2S gradients revealed by these microsensors and their correlation to other solute distributions have provided great insights into the biogeochemical pathways of sulfate reduction, sulfide oxidation, and related trace element cycling and transport in deposits. The microsensors can be moved through deposits along linear

tracks and provide one-dimensional vertical profiles which cannot resolve lateral variability in H_2S distributions without repeated deployments.

Two-dimensional measurements of total sulfide in sediments have been pioneered by using DGT (diffusive gradients in thin-films) techniques (Teasdale et al., 1999; Devries and Wang, 2003; Jézéquel et al., 2007; Robertson et al., 2008). In this application, a passive equilibrator is comprised of two polyacrylamide hydrogel layers backed by a glass plate. The inner layer incorporates a sulfide binding agent, AgI, and the outer layer is a diffusive gel of well-defined thickness that both protects the inner gel and allows for calculation of sulfide fluxes corresponding to the accumulation of AgS product over a known time (Davison et al., 2000; Robertson et al., 2008). The accumulated total sulfide in the binding gel is measured using computer-imaging densitometry. A composite trace metal and sulfide DGT device has also been reported, and utilizes an outer layer diffusive gel as DET (diffusive equilibrium in thin-films) sampler for simultaneously measuring 2-dimensional metals and sulfide in sediments (Motelica-Heino et al., 2003; Naylor et al., 2004; Jézéquel et al., 2007; Robertson et al., 2008). Although the DGT technique has been used for measuring 2-dimensional distribution patterns of total sulfide and provided new insights into sulfide heterogeneity in marine sediments, it is not suitable for the study of reaction dynamics because of its irreversible response, relatively long deployment time (> 10 hours), and ex situ measurement of Ag_2S in binding gel.

Planar optical sensors are alternative approaches for 2-dimensional measurements, and have been used to quantify 2-dimensional distributions of various porewater solutes such as O_2, pCO_2, NH_4^+, pH and Fe^{2+} in heterogeneous marine sediments with high spatial and temporal resolution (Glud et al., 1996; Wenzhöfer and Glud, 2004; Stromberg and Hulth, 2001, 2003; Zhu et al., 2005, 2006a,b, 2010; Schröder et al, 2007; Zhu and Aller, 2012). However, a planar

optical sensor for 2-dimensional measurement of H_2S has not been reported. In this paper, we propose a new planar fluorosensor for 2-dimensional H_2S measurement by using Pyronin Y (PY) as a H_2S indicator to reveal 2-dimensional hydrogen sulfide distribution patterns and dynamics in bioturbated salt marsh sediments.

2. Materials and Methods

2.1. Preparation of H_2S fluorosensor foils modifications M1 and M2

The H_2S planar fluorosensor membranes were fabricated by physically immobilizing Pyronin Y (Sigma-Aldrich) in a thin film of hydrophobic ethyl cellulose (Sigma-Aldrich). The sensing membranes are backed by an inert transparent Mylar polyester sheet (0.005 inch thick, Ridout Plastics) and covered by a gas permeable silicone membrane to eliminate the interferences of hydrated ions.

The membrane modification M1 cocktail was prepared by mixing 8.0 ml of 2% ethyl cellulose solution in ethanol/toluene (10/90, v/v) and 0.5 ml of 1.0 mg/ml PY solution in ethanol. The mixture was gently stirred for 5 min at room temperature (~ 22° C) and cast on a level transparent polyester sheet (300 cm^2). The wet foil was covered by a glass tray with ~0.5 cm space above the sensor sheet. After slow evaporation of the solvent for 3 hours in a hood, the dry ethyl cellulose membrane has a thickness of roughly 10 μm. A thin layer of silicone rubber solution (silicone rubber Dow Corning 3140 diluted with benzene/xylene (2/5, v/v)) was then applied on the sensing membrane and was rapidly evaporated with a hair dryer. The sensor foil was cured for 1 day in a hood and soaked in water for 20 min prior to use.

The membrane modification M2 cocktail was prepared by mixing 8.0 ml of 2% ethyl cellulose solution in ethanol/toluene (10/90, v/v) and 0.1 ml of 1.0 mg/ml PY solution in ethanol. The sensor foil fabrication method is otherwise the same as M1.

2.2. Optical Instrumentation

Fluorescence excitation and emission spectra, response time, dynamic range and fabrication optimization of the sensor were performed on a Hitachi F-4500 fluorescence spectrophotometer. A sensor foil cuvette and holder were home-made for directly measuring the fluorescence of a membrane in solution or contacting solid sediment samples. Incidence light angle was set at 30º and emission light angle at 60 º in order minimize the reflected light from excitation. Unless otherwise stated, all measurements were performed at room temperature (~22ºC).

Two-dimensional fluorescence image measurements were carried out on a home-made fluorescence imaging system (Fig. 1). The light source is a monochromator (Oriel Spectral Luminator) equipped with a 150-W Xe UV/VIS arc lamp and controlled by computer. The detection system is composed of an emission filter wheel and a digital camera (Canon EOS 10D, 2048×3072 pixels). A Canon lens model EF-100 mm and Canon Remote Capture software 2.7 were used to collect fluorescence images, and an emission filter with 577 nm (bandwith 10 nm; Intor, Inc.) was used to cut off reflected or scattered light. Reflected light was further eliminated by using an excitation incident angle of 30° and emission measuring angle of 90°. Image analysis and data calculations were performed with Maxim DL image processing software version 2.0X (Diffraction Limited) and Image-Pro plus version 4.1 for Windows (Media Cybernetics). Images were split into blue, green and red bands and the red band was used to calculate the intensities of

individual pixels. Background noise was very low for a range of sediment types of varied color (dark gray to black), and is included within the analytical uncertainty of <5%.

2.3. Sensor Calibration

Hydrogen sulfide is an acid gas and can slightly dissolve in water to form a weakly acidic solution. The dissolved hydrogen sulfide is involved in the following dissociation reactions in water:

$$H_2S(aq) \xleftrightarrow{K_1} HS^-(aq) + H^+(aq)$$

$$HS^-(aq) \xleftrightarrow{K_2} S^{2-}(aq) + H^+(aq)$$

Where K_1 (pK_1=6.88) and K_2 (pK_2=14.15) (Greenwood and Earnshaw, 1986) are the first dissociation constant and second dissociation constant of the hydrogen sulfide system at infinite dilution, respectively. The apparent or conditional pK_1' in seawater (35 salinity; T = 25° C) is 6.5-6.6 (Millero et al, 1988). Assuming the conditional constants for seawater (or the thermodynamic constants with activity coefficients unity), the total sulfide (ΣH_2S) and the concentration of hydrogen sulfide can be written as (Kühl et al, 1998):

$$\sum H_2S = [H_2S] + [HS^-] + [S^{2-}]$$

$$[H_2S] = \frac{\sum [H_2S]}{1 + \frac{K_1'}{[H^+]} + \frac{K_1'K_2'}{[H^+]^2}} \qquad (1)$$

If the amount of total sulfide is fixed, the concentration of hydrogen sulfide only depends on the ambient pH according to the Eq. (1). When the ambient pH is less than 4, over 99.9% of total sulfide is in the form of H_2S in the solution. At pH=6.5 (pK_1') in seawater, the concentration of

molecular H_2S equals the HS^- concentration. At pH=9, the predominant form of hydrogen sulfide species is the HS^-, higher than 99% of total sulfide.

Because the natural pH value in marine sediment is generally in the range of 6 to 7.5, calibration standards for dissolved hydrogen sulfide were made from a pH 6.88 phosphate buffer (0.01M) in sealed cuvettes, for constructing a calibration curve using the imaging system. Sodium sulfide solutions were freshly prepared before use by dissolving appropriate amounts of $Na_2S{\cdot}9H_2O$ (Fisher Sci.) in oxygen free deionized and distilled water. A small piece of subsample of a sensor foil were mounted on the inside front face of a 4-mL plastic cuvette and immersed in 2 ml oxygen free phosphate buffer (N_2 purged). After sealing the cuvette, 50 μl of sodium sulfide standard solution was injected into the buffer. The H_2S concentration was calculated using Eq. (1), and the fluorescence intensity of the sensor strip was measured using the camera system as mentioned previously. The fluorescence quenching extent, F_0/F, was utilized to construct a calibration against the concentration of hydrogen sulfide, where F_0 and F are the average fluorescence intensities of a sensor foil in the absence and presence of hydrogen sulfide, respectively.

For the experiments performed using the Hitachi F-4500 fluorescence spectrophotometer, such as optimization of sensor fabrication, response time and dynamic range measurements, hydrogen sulfide was generated in a 0.1 M HCl solution in the sealed home-made cuvette.

2.4. Sediment samples

Sediment box cores (12×30×30 cm) and seawater were collected from intertidal mudflat sites in Flax Pond, a salt marsh on the northshore of Long Island, New York, USA. No plant and grass rhizomes were present in the sediments. The intact cores were immediately transferred to

the laboratory and incubated in a tank (filled with seawater from the sample site) at room temperature (22°C) with constant aeration of overlying water (salinity = 28). The overlying water and the upper ~15 cm of the sediments were subcored for the 2-dimensional H_2S measurements. The concentrations of porewater ΣH_2S and Fe^{2+} at this site are typically around 2 – 8 mM (Swider and Mackin, 1989) and 10 - 100 μM (Swider and Mackin, 1989; Zhu and Aller, 2012), respectively.

2.5. Two-Dimensional H_2S distribution measurements

A small rectangular corer (6×15×20 cm) with two glass faces, two acrylic faces, and two open ends was used for subcoring the intact sediment in the larger boxcore and for subsequent measurement of 2-D H_2S distributions. Two H_2S sensor foils (14×15 cm) were installed on the inside of the front- and back- glass faces of the subcorer before it was gently inserted into the salt marsh sediment. After sealing the bottom and cleaning the outside, the subcore was put back in the seawater container and continuously aerated for 1 hour at room temperature in the dark before fluorescence images were taken. The excitation wavelength was set at 554 nm, and an emission filter with 577 nm (± 10 nm) was chosen for fluorescence imaging.

In order to determine the effect of bioturbation and biogenic structure on H_2S distribution patterns, 5 individual *Nereis succinea* (the common rag worm present at the sample site) with lengths of 6 ~ 10 cm were added into the sediment microcosm after the undisturbed intact 2-dimensional H_2S distribution pattern was measured. H_2S fluorescence and visible images were then obtained at 1, 3, 5, 12, 24, and 48 hours. During imaging, a black plastic film was vertically inserted in the overlying water in the middle of the microcosm as mentioned above.

3. Results and Discussion

3.1 Fluorescence Spectra of Sensors

Pyronin Y is a cationic, water soluble xanthene derivative that has been widely used in histochemistry as nucleic acid stain (Kapuscinski and Darzynkiewicz, 1987). The free dissolved PY molecule shows bright fluorescence in aqueous solution with an excitation maximum at 548 nm and corresponding emission 566 nm, which can be significantly quenched by addition of sulfide/bisulfide ion (Fig. 2A). When PY was physically entrapped in an ethyl cellulose membrane and covered with a gas permeable silicone membrane, the fluorescence spectra of immobilized dye showed similar excitation and emission bands to those of free PY in solution but with a slight red shift. The emission maximum of the sensor membrane red-shifted 1 nm, and the excitation maximum red-shifted to 554 nm from 548 nm. The excitation spectrum also became broader than that of free PY spectrum in water. The slight red shifts and deformation of the fluorescence spectra of immobilized PY might be caused by the H-aggregate of PY molecules in the sensing membrane due to its high concentration in the solid phase (Alanyalioglu and Arik, 2009). The immobilized PY in the sensor foil did not respond to sulfide and bisulfide ions in contacting solution but specifically to hydrogen sulfide because the outer layer gas-permeable silicone membrane blocked all hydrated ions. When the sensor foil was immersed in hydrogen sulfide solution, dissolved gaseous hydrogen sulfide diffused through the silicone membrane and caused a fluorescence decrease of the immobilized PY (Fig. 2B). Compared to the response of free PY to sulfide/bisulfide in solution, the sensor foil is less sensitive to hydrogen sulfide. This phenomenon may be explained by the relatively high PY concentration in the sensor membrane.

3.2 Sensor Fabrication

Gas sensing optical foils are generally comprised of an outer layer gas permeable membrane to eliminate interferences from hydrated ions and to protect the inner sensing film from direct contact with solutions. The indicator compound can therefore be physically incorporated into the inner sensing membrane without leakage based on the simplest physical immobilization methods. In order to obtain a large uniform sensor film suitable for fast and sensitive mapping of 2-dimensional hydrogen sulfide distribution in sediment, the polymer matrix material, indicator concentrations in the sensor membrane, and the membrane thickness were optimized.

Hydrophobic and hydrophilic polymer materials were compared for the sensor performance by incorporating the same amounts of PY into ethyl cellulose and D4 polyurethane (Hydromed) hydrogel membrane. Results showed that the immobilized PY emitted strong fluorescence in both sensing membranes, but it almost completely lost its response to hydrogen sulfide in the hydrophilic D4 membrane (data not shown). In contrast, PY fluorescence in ethyl cellulose membrane was significantly quenched in the presence of hydrogen sulfide, and ethyl cellulose was therefore chosen in this work. Other advantages of an ethyl cellulose polymer carrier include: non-fluorescence, UV-Vis range transparency, high gas permeability, easy fabrication and adequate mechanical strength for sediment applications. Polyester Mylar plastic sheet was selected as a backing support material for the ethyl cellulose membrane because of its excellent stability for adhering to the sensing membrane, mechanical flexibility and rigidity (easy to insert into sediment), UV-Vis range light transparency, and chemical resistance. Silicone rubber is an excellent gas permeable water barrier for planar gas-sensors (e.g., Zhu et al, 2006b, 2010). In this work, a room temperature curing silicone rubber Dow Corning 3140 was chosen as the outer

protective layer because no acidic substances were released into the sensor membrane during curing. The thickness of the silicone membrane was controlled in the range of 5 – 10 μm. A thicker silicone membrane would better protect the inner sensing membrane but prolong the gas transport time and thus increase the overall response time. A thinner silicone membrane would not affect sensor response time but could be easily scratched and penetrated by large sediment particles during insertion into sediment.

The thickness of the inner ethyl cellulose sensing membrane was optimized by fixing the protective silicon membrane thickness at 5 – 10 μm. The results showed that the response time was directly proportional to the sensing membrane thickness when the amount of ethyl cellulose on a 300 cm^2 sensor sheet increased from 4 ml to 16 ml of 2% polymer solution (~5 to 20 μm thick). On the other hand, when the amount of ethyl cellulose was less than 4 ml of 2% solution per 300 cm^2, it was too thin to completely immobilize indicator over a uniform large membrane. For application in marine sediments, 8 ml of 2% ethyl cellulose solution was chosen to prepare a stable 300 cm^2 sensing membrane with a rough thickness of 10 μm.

Indicator PY concentration in the solid sensing membrane was also studied. Our results showed that the fluorescence signal, response time and dynamic range decreased but sensitivity increased as the immobilized amount of PY decreased. Therefore, the optimal amount of immobilized PY in a sensor foil should be determined by the analyte concentration, and is a compromise between response time, sensitivity, analytical dynamic range, and camera sensitivity. For sensor applications in salt marshes with relatively high hydrogen sulfide concentrations (0.1 – 5 mM), sensor modification M1, fabricated by homogeneously immobilizing 500 μg PY in 300 cm^2 ethyl cellulose film, is optimal because it exhibits a wide dynamic working range (over 3 mmol/L H_2S) and a suitable response time (discussed below). On the other hand, sensor

modification M2, which is prepared by immobilizing 100 μg PY in 300 cm^2 ethyl cellulose film, is better for measuring low level H_2S in sediments and other samples due to its higher sensitivity, reversibility, and narrower dynamic working range.

The final sensor foils were transparent and uniform, and showed bright fluorescence at 567 nm with excitation maximum at 554 nm. The sensor foil was immersed in water for about 20 min prior to application. Sensor foils can be sealed in a plastic bag and stored in the dark at room temperature for at least 1 year.

3.3 Sensor Response Characteristics

The reaction mechanism between PY and hydrogen sulfide has not been specifically studied, however, we hypothesize that the fluorescence quenching of PY is caused by the formation of PY^+HS^- ion pairs in the presence of hydrogen sulfide (Fig. 3). PY^+ has several resonance structures, with C or N atoms bearing the positive charge (Reija et al., 2005). Because C^+ shows greater electron withdrawing ability than N^+, the nucleophile bisulfide may attack positive carbon to form the PY^+HS^- ion pair, causing the breakdown of the π-π conjugate system and fluorescence quenching. If the concentration of H_2S in solution is lowered, H_2S in the membrane diffuses out, resulting in the dissociation of the PY^+HS^- ion-pair and fluorescence recovery. This hypothesis is supported by the reversible (or semi-reversible) response of the sensor to various H_2S concentrations in the complete absence of oxygen or other oxidant. The results in Figure 4A show that the sensor fluorescence was quenched by adding H_2S and clearly responded to different H_2S concentrations. Because no oxygen was present in this system, the recovery of sensor fluorescence may be caused by the dissociation of the hypothesized PY^+HS^- ion-pair rather than re-oxidation of reduced PY. Assuming the ion-pair mechanistic scheme, the

production of reactant bisulfide nucleophile within the sensor foil will cause a pH decrease (H_2S dissociation in Fig. 3). The accumulation of excess protons within the sensor foil would result in less H_2S dissociation in the membrane and presumably degrade sensor reversibility after multiple measurements at high H_2S.

The proposed reaction mechanism of PY with H_2S is different from other H_2S optical indicators such as methylene blue and thionine, which are produced from the reaction of aqueous sulfide and N, N-dimethylphenyl-1,4-diamine or its derivatives in the presence of ferric ions (Lawrence et al., 2000). These reactions are irreversible. On the other hand, methylene blue and thionine have also been used directly as indicators in kinetic protocols for sulfide detection. In these cases, the oxidized form (colored) of the chromogen can be reduced to a colorless form by sulfide in the presence of trace amounts of Cu or Se ion as catalyst. The colorless products can be oxidized by oxygen to regenerate their colored oxidized form (Kohls et al., 1996; Shamsipur et al., 2005). However, the process of chromagen regeneration is very slow. The regeneration time is found to be 30 – 60 min at low sulfide concentration (<0.1 mM), but over 15 hrs in high sulfide concentration (>10 mM) (Shamsipur et al., 2005). In addition, the presence of metal ion catalyst makes optical sensor fabrication and application complicated. Optical sensors based on these chromagens are not very suitable for in-situ H_2S measurements in sediments.

The response time of fluorosensor M1 to hydrogen sulfide at room temperature was evaluated by alternately dipping the sensor foil in a solution without H_2S and a solution containing 550 μM dissolved H_2S at pH = 6.88. When a fresh sensor foil was immersed in H_2S free solution at room temperature, the fluorescence intensity at 567 nm continuously increased for about 15 min and then reached a constant maximum. We presume that this increased sensitivity was due to diffusion of water vapor and hydration of PY in the inner sensing

membrane, generating higher fluorescence emission closer to that of free solution. Therefore, for maximum and stable sensitivity, sensor foil needs to be equilibrated in H_2S free water for ~20 min prior to use. When conditioned sensor foil was immersed in 550 μM H_2S solution, fluorescence intensity sharply decreased. It can be seen from Figure 4B that it takes about 1 min to reach 90% response (t_{90}) and 2 min to reach almost 100% equilibrium. For the fluorescence recovery of the sensor in H_2S free solution, 90% recovery (R_{90}) was obtained at 30 seconds and full equilibrium was reached at ~1 min. However, we found that the first cycle response was not completely reversible; the fluorescence recovery reaction in H_2S free solution did not reach the same fluorescence intensity as the initial signal. After the first cycle, the sensor response seems to be reversible with t_{90} 1 min and r_{90} 30 seconds. For practical application, one cycle sensor response in a 550 μM H_2S solution was performed prior to deploying the sensor foil into sediments. The operational reproducibility of the sensor was further studied by repeatedly changing hydrogen sulfide concentration from 0 to 550 μM, and then back to 0 μM. The results indicated that the fluorescence quenching extent (F_0/F) decreased after 5 – 6 response cycles, implying the sensor foil may be deployed for approximately 5 cycles in highly sulfidic sediment. Otherwise, relatively high measurement error could be introduced.

It was found that the sensor performance such as sensitivity, response time, and response dynamic range were closely related to the immobilized indicator amount. The response time, sensitivity and reversibility could be improved by decreasing the immobilized PY in the membrane. When the immobilized PY was lowered to 100 μg per 300 cm^2 (M2 sensor), the sensor response to low level H_2S was almost completely reversible (Fig. 4C). The sensor fluorescence decreased in the presence of 12.5 μM H_2S, however, it recovered to essentially the

original fluorescence intensity when the sensor was immersed in H_2S free solution. The response time of M2 was also improved to 15 s.

The quantification of hydrogen sulfide using sensor modification M1 was studied by immersing a small piece of sensor foil M1 into pH 6.88 phosphate buffer with various hydrogen sulfide concentrations in a sealed cuvette. The fluorescence intensity at 567 nm was inversely correlated with the dissolved H_2S concentration, and the extent of fluorescence quenching (F_0/F) showed a good linearity versus the concentration of hydrogen sulfide in the range of nd – 3150 μM (higher concentrations were not tested) (Fig. 5A). The broad analytical dynamic range is suitable for hydrogen sulfide quantification in sulfidic deposits such as salt marshes. The detection limit calculated from the standard deviation of blank (3σ) was 40 μM, implying that the formulation of the M1 sensor is not sensitive enough to measure low level H_2S. Generally, the fluorescence quenching is governed by Stern-Volmer equation:

$$\frac{F_0}{F} = 1 + K_{SV}[Q]$$

where F_0 and F are the fluorescence intensity in the absence and presence of quencher, K_{sv} is Stern-Volmer quenching constant, and [Q] is quencher concentration. The results shown in Fig. 5A indicate that the sensor calibration equation of the best-fit line, $F_0/F = 1.061 + 0.0006[H_2S]$, matches the Stern-Volmer equation with K_{sv}=0.0006. In order to obtain high accuracy and precision of H_2S quantification, a subsample of each sensor foil was calibrated along with sample measurement. Compared with the M1 sensor, low level H_2S sensor M2 also follows the Stern-Volmer relation with a K_{sv} =0.0083 but F_0/F exhibits a much narrower dynamic range (nd – 50 μM) against H_2S concentration. Nevertheless, fluorescence quenching (F_0-F) shows a wide

linearity with H_2S concentration in the range from nd to 125 μM H_2S with a detection limit of about 4 μM (3σ) (Fig. 5B).

Compared to electrochemical H_2S microsensors (e.g. Kühl et al., 1998), the detection limits of the M1 and M2 sensors are not low. Nevertheless, the planar sensors are appropriate to quantify levels of H_2S observed in sulfidic sediments such as salt marsh deposits due to the wide dynamic working range, and to measure 2-D H_2S distribution patterns associated with biogenic/abiogenic sedimentary structures. Because the planar sensor foils only respond to dissolved H_2S, the fluorescence response for the same total sulfide will decrease with increasing pH value due to the dissociation of H_2S to ionic bisulfide and sulfide, which are blocked by the silicone membrane. However, the fluorescence response decrease at higher pH would not change the sensor sensitivity towards H_2S per se, which is an inherent sensor parameter.

The operational stability was evaluated by continuously exciting the sensor foil at 554 nm for 60 min, no photobleaching was observed. The sensor response stability was also tested by storing the sensor foil in a sealed plastic bag in dark at room temperature. Our results showed that the sensor blank fluorescence intensity and sensor response to hydrogen sulfide were essentially constant for at least 1 year (longer times were not tested).

3.4 Interferences

In the proposed fluorescence sensor foil, the inner sensing membrane is protected by the outer layer silicone film which is gas permeable. Therefore, the potential interferences from various nonvolatile inorganic and organic cations and anions in the solution can be completely eliminated. The primary gases present in sediment such as O_2, N_2, CO_2, and NH_3 can also cross through the silicone membrane, the effects of these dissolved gases on the sensor response was

studied. The results, summarized in Table 1, indicate that these dissolved gases do not have an impact on the sensor response even when they are present in very high concentrations.

3.5 Two-dimensional H_2S distributions in vertically stratified sediment

A two-dimensional H_2S distribution pattern in intact salt marsh sediment was measured using the sensor. A sediment core was collected from intertidal mudflat site in Flax Pond on September 24, 2007 and imaged the same day. Macrofaunal population abundances were depleted at the time of sampling, and the sediment physical features were close to being vertically stratified (Fig. 6A). The sediment showed a very flocculent surface, and oxygen penetrated to a depth of ~5 mm into the flocculent layer. The corresponding 2-dimensional H_2S distribution pattern revealed by the sensor showed the vertically stratified H_2S distribution in this sediment (Fig. 6B). The H_2S concentration was non-detectable (nd) in the overlying water, and within the oxic layer of the sediment, but it increases dramatically below the oxic-anoxic interface. A thin H_2S diffusive boundary layer can be clearly seen at the oxic-anoxic interface, indicating that hydrogen sulfide is completely oxidized in the oxic sediment layer by chemical oxidation (e.g., O_2, NO_3^-, Mn and Fe oxides) (Jørgensen and Nelson, 2004) or sulfide-oxidizing bacteria. The amount of H_2S transported from anoxic sediment to the oxic zone is balanced by these H_2S oxidation processes, resulting in no detectable flux of H_2S to the overlying water. Below the oxic-anoxic interface, H_2S can also be oxidized by secondary oxidants such as NO_3^-, MnO_2 and FeOOH in the anoxic zone (Morse et al., 1987; Jørgensen and Gallardo, 1999; Poulton et al., 2004; Yücel et al., 2010; Luther et al., 2011). The steep gradient of H_2S from 0.5 cm to 2 cm is evidence of these suboxic oxidation reactions. The concentration of H_2S reaches a maximum at a depth of about 2 cm and remains almost constant down to 10 cm below the

sediment surface (deeper sediment was not tested), reflecting the production of hydrogen sulfide from extremely intensive sulfate reduction regulated by sulfate-reducing bacteria in the deeper sediment (Berner, 1963; Morse et al., 1987; Brüchert et al., 2003). Figure 6B also shows that although the H_2S overall distribution pattern is close to being vertically stratified, and its concentration is almost homogeneous below 2 cm depth, microniches with elevated H_2S are clearly visible. These high H_2S "hotspots" are likely caused by spatially discrete aggregates of sulfate-reducing bacteria and labile organic matter (Devries and Wang, 2003).

3.6 Spatial and Temporal 2-D H_2S distributions in bioturbated sediments

Coastal marine deposits are generally not well stratified within the surficial zone due to the presence of macrobenthos. The activities of bottom dwelling macrofauna can generate complex three dimensional biogeochemical reaction patterns over millimeter to meter scales below the sediment surface (Aller, 1982, 2001; Kristensen, 1988; Kristensen and Kostka, 2005). In order to evaluate the spatial and temporal 2-D hydrogen sulfide distribution patterns in bioturbated sediments, 5 *Nereis succinea* (the common rag worm present at the sample site) with lengths of 6 to 10 cm, were added into a vertically stratified sediment microcosm, and the 2-D hydrogen sulfide distributions were measured using the planar sensor at 1, 3, 5, 12, 24 and 48 hours. Figure 7 directly shows the complex spatial and temporal patterns of H_2S that can be generated in bioturbated sediments. Burrows were quickly constructed when the *N. succinea* were introduced into the microcosm. H_2S concentrations in well irrigated burrows are low or nd, and a sub-boundary around the burrows can be clearly seen. The rightmost burrow in Figure 7 was formed within 1 hour and retained a stable shape for 24 hours while the worm intermittently utilized it. Burrows in the middle of the microcosm were formed and abandoned in succession, and the H_2S

distributions dynamically followed the change in physical structure of sediment and animal activity. H_2S plumes exiting from actively irrigated burrow sections can occasionally be seen (Fig. 7A'-D'), demonstrating that reduced sedimentary solutes can be directly exchanged and advectively mixed with oxygenated overlying water during irrigation, with the burrows acting as conduits. On the other hand, H_2S concentrations in the sections of abandoned and infilled burrows are clearly higher than that in the surrounding environments (Fig. 7D'-F'). The increased concentration of hydrogen sulfide associated with relict biogenic structures could be caused by: (1) Additional organic matter such as mucus secretions are elevated in the vicinity of burrows and may act as sites of enhanced microbial activity, including SO_4^{2-} -reduction (Aller, 1982, 2001; Kristensen, 1988; Kristensen and Kostka, 2005). (2) Elevated decomposition generates additional acids and CO_2 in the abandoned and infilled burrows (Zhu et al., 2006a, b), which would result in lower pH and more dissolved bisulfide converting to H_2S based on equation (1). The high H_2S regions associated with such burrow fill and relict biogenic structures dissipate after approximately 12 - 24 hours (Fig. 7D'-F'). This relaxation phenomenon is direct evidence for the eventual re-equilibration of stagnant voids created by macrofauna with surrounding sediment. The local increases and decreases of H_2S respectively associated with abandoned and inhabited burrows create a complex, time dependent and three-dimensional pattern of H_2S distribution and associated reactions in marine sediment, all of which are a function of faunal size, abundance, burrowing and irrigating activities.

As the speciation of H_2S is closely coupled to pH values of samples, elevated acids in the abandoned and refilled burrows may be a major reason for the spatial variations of H_2S in Figure 7D'-F' . Our previous study showed that pH values were in the range of 5.8 – 7 in the sediments collected from the same site (Zhu et al., 2006a). A small scale pH decrease in this pH range

could cause a significant H_2S increase based on eq (1) even when the total sulfide concentration remains the same. Therefore, a single H_2S planar sensor cannot provide sufficient information for studying total sulfide in sediment, and a planar pH sensor should be coupled to the H_2S sensor for accurate speciation and concentration measurements. Sequential measurements of pH and H_2S in sediment by switching the two single planar sensor foils can provide two separate 2-dimensional pH and H_2S distributions which could be used to calculate 2-dimensional total sulfide distribution in a well sorted and stratified sediment. However, the fine structure of complex biogenic features in bioturbated sediment could be modified during sensor foil switching. The separate 2-dimensional pH and H_2S distributions may not reflect their spatial and temporal coupling, and may generate significant artifacts during total sulfide calculations. This issue can be addressed by simultaneously measuring 2-dimensional pH and H_2S using a composite planar sensor.

The heterogeneity of H_2S distribution in bioturbated sediment was further quantified by calculating the minimum, maximum and average vertical H_2S profiles (Fig. 8A), as well as the horizontal distribution pattern in sediment (Fig. 8B), using the distribution pattern at 12 hours shown in Figure 7D' as an example. It can be seen that although the average vertical H_2S profile in the bioturbated sediment is similar with that in stratified sediment shown in Fig. 6C, the H_2S concentration variations between the maximum and minimum values are in the range of nd – 3850 μM H_2S from sediment surface to 7 cm depth. A horizontal transect at 2.5 cm (Fig. 8B) shows that the concentration of H_2S can decrease from 5000 to 1000 μM over a distance of 0.5 cm dictated by the spacing of irrigated burrows, and can oscillate between 1000 and 5000 μM even in the same horizontal sediment layer (Fig. 7, Fig. 8B). These results readily demonstrate the significant variability of H_2S distributions in bioturbated sediment, and the limitation of

traditional methods for quantification of biogeochemical reactions, authigenic mineral formation, and associated processes in the bioturbated zone.

4. Conclusions

Planar fluorosensors for measuring 2-dimensional H_2S distributions in marine sediment were developed based on pyronin Y. The sensor modification M1 has a response time of ~ 1 min and a working dynamic range of nd - 3150 μM H_2S, which is very suitable for H_2S quantification in highly sulfidic sediments such as salt marshes or in sediments with low reactive Fe such as carbonates. The sensor configuration M1 utilized here is suitable for high H_2S and is moderately reversible; losing its response after 5 – 6 measurement cycles. Sensor modification M2 is more sensitive and reversible, and is suitable to measure low level H_2S in sediments (nd – 125 μM). By using commercially available digital cameras, sub-millimeter resolution can be readily achieved. This transparent sensor has been successfully applied to study spatial and temporal 2-dimensional H_2S distributions. Complex, time-dependent and multi-dimensional H_2S distribution patterns and related biogeochemical reaction dynamics are associated with burrow construction, scaling, and irrigation activity, and were directly revealed and documented for the first time. Combined with other planar optical sensors such as O_2, pH and pCO_2 sensors, these fluorosensors provide powerful options for the study of sulfur biogeochemistry and cycling in marine sediments.

Acknowledgements

We thank G. W. Luther for constructive comments, particularly on possible reaction mechanisms. This work was supported by the US National Science Foundation (OCE0851207, OCE0526410 and OCE0752105).

References

Alanyalioglu, M. and Arik, M., 2009. Electrochemical preparation of pyronin Y thin films on gold substrates. J. Appl. Poly. Sci. 111: 94–100.

Aller, R.C., 1982. The effects of macrobenthos on chemical properties of marine sediment and overlaying water. In Animal-sediment relation, P. L. McCall and M. J. S. Tevesz (eds.). Plenum. pp. 53-102.

Aller, R.C., 2001. Transport and reactions in the bioirrigated zone. In The Benthic Boundary Layer, B. P. Boudreau and B. B. Jørgensen (eds.). Oxford Univ. Press, Oxford. pp. 269–301.

Aller, R.C., Madrid V., Chistoserdov, A., Aller, J.Y. and Heilbrun, C., 2010. Unsteady diagenetic processes and sulfur biogeochemistry in tropical deltaic muds: implications for oceanic isotope cycles and the sedimentary record. Geochim. Cosmochim. Acta 74, 4671-4692.

Berner, R.A., 1963. Electrode studies of hydrogen sulfide in marine sediment. Geochim. Cosmochim. Acta 27:563-575.

Berner R.A., 1984. Sedimentary pyrite formation: An update, Geochim. Cosmochim. Acta 48: 605-615.

Brendel, P. and Luther, G.W., 1995. Development of a gold amalgam voltammetric microelectrode for the determination of dissolved Fe, Mn, O2 and S(-2) in porewaters of marine and freshwater sediments. Environ. Sci. Technol. 29:751–761.

Brüchert V., Jørgensen B.B., Neumann K., Riechmann D., Schlösser M., Schulz H., 2003. Regulation of bacterial sulfate reduction and hydrogen sulfide fluxes in the central Namibian coastal upwelling zone, Geochim. et Cosmochim. Acta, 67(23): 4505-18,

Canfield, D.E., 2004. The evolution of the Earth surface sulfur reservoir. Am. J. Sci. 304: 839-861.

Canfield, D.E., Raiswell, R., Bottrell, S., 1992. The reactivity of sedimentary iron minerals toward sulfide. Am. J. Sci. 292:659-683.

Choi, M.M.F. and Hawkins, P., 2003. Development of an optical hydrogen sulphide sensor. Sensors and Actuators B, 90:211-215.

Ciglenecki, I. and Cosovic, B., 1996. Electrochemical study of sulfur species in seawater and marine phytoplankton culture. Mar. Chem. 52: 87-97.

Cline, J.D., 1969. Spectrophotometric determination of hydrogen sulfide in natural water. Limnol. Oceanogr. 14:454-548.

Davison, E., Fones, G., Harper, M., Teasdale, P. and Zhang, H., 2000. Dialysis, DET and DGT: in situ diffusional techniques for studying water, sediments and soils, In J. Buffle and G. Horvai (Eds.), In situ monitoring of aquatic systems: chemical analysis and speciation. Wiley. pp. 495-569.

Devries, C. and Wang, F., 2003. In situ two-dimensional high resolution profiling of sulfide in sediment interstitial waters. Environ. Sci. Technol. 37(4):792-797.

Glud, R.N, Ramsing, N.B., Gundersen, J.K. and Klimant, I., 1996. Planar optrodes: a new tool for fine scale measurements of two-dimensional O_2 distribution in benthic communities. Mar. Ecol. Prog. Ser. 140: 217–226.

Goldhaber, M.B. and Kaplan, I.R., 1975. Controls and consequences of sulfate reduction rates in recent marine sediments. Soil. Sci. 119: 42-55.

Greenwood, N.N. and Earnshaw, A., Chemistry of the elements. Pergamon, Oxford, 1986, p.807.

Jézéquel, D., Brayner, R., Metzger, E., Viollier, E., Prévot, F. and Fiévet, F., 2007. Two-dimensional determination of dissolved iron and sulfur species in marine sediment pore water by thin-film based imaging. Thau lagoon (France). Estuarine, Coastal and Shelf Science 72: 420-431.

Johnston, D.T., 2011. Multiple sulfur isotopes and the evolution of Earth's surface sulfur cycle. Earth-Science Reviews 106:161-183.

Johnson, K.S. and Coletti, L.J., 2002. In situ ultraviolet spectrophotometry for high resolution and long-term monitoring of nitrate, bromide and bisulfide in the ocean. Deep-Sea Res. I 49: 1291-1305.

Jørgensen, B.B and Kasten, S., 2006. Sulfur cycling and methane oxidation. In: Marine Geochemistry, 2nd Ed. (H.D. Schulz and M. Zabel, eds.). Springer – Verlag, Berlin. 271-309.

Jørgensen, B.B. and Gallardo, V.A., 1999. Thioploca spp: filamentous sulfur bacteria with nitrate vacuoles. FEMS Microbiol. Ecol. 28, 301–313.

Jørgensen, B.B. and Nelson, D.C., 2004. Silfide oxidation in marine sediments: Geochemistry meets microbiology. In Amend, J.P., Edward, K.J., and Lyons, T.W., eds. Sulfur Biogeochemistry – Past and Present: Geological Society of America Special Paper 379, pp. 63-81.

Kapuscinski , J. and Darzynkiewicz, Z., 1987. Interactions of Pyronin Y(G) with nucleic acids. Cytometry 8:129-137.

Kohls, O., Klimant, I., Holst, G.A. and Kühl, M., 1996. Thionine as an indicator for use as a hydrogen sulfide optode. Proc. SPIE, 2836:311-321.

Kristensen, E., 1988. Benthic fauna and biogeochemical processes in marine sediments: microbial activities and flux. In Nitrogen cycling in coastal marine environments, T. H. Blackburn and J. Sørensen (eds.). Wiley, New York. pp. 275-299.

Kristensen, E. and Kostka, J.E., 2005**.** Macrofaunal burrows and irrigation in marine sediment: microbiological and biogeochemical interactions. In: Interactions between Macro- and Microorganisms in Marine Sediments, E. Kristensen, J.E. Kostka, R. Haese (edit's), American Geophysical Union, Washington, DC, 390 pp.

Kuban, V, Dasgupta, P.K. and Marx, J.N., 1992. Nitroprusside and Methylene Blue Methods for Silicone Membrane Differentiated Flow Injection Determination of Sulfide in Water and Wastewater. Anal. Chem. 64:36-43.

Kühl, M., Steuckart, C., Eickert, G., Jeroschewski, P., 1998. A H_2S microsensor for profiling biofilms and sediments: application in an acidic lake sediment. Aquat. Microb. Ecol. 15:201-209.

Lawrence, N.S., Davis, J., Compton, R.G., 2000. Analytical strategies for the detection of sulfide: a review. Talanta, 52:771-784.

Luther III, G.W., Giblin, A.E. and Varsolona, R., 1985. Polarographic analysis of sulfur species in marine porewaters, Limnology Oceanography 30, 727-736.

Luther III, G.W., Church, T.M., Scudlark, J. and Cosman. M., 1986. Inorganic and organic sulfur cycling in salt marsh porewaters, Science 232, 746-749.

Luther, III, G.W., Brendel, P.J., Lewis, B.L., Sundby, B., LeFrançois, L., Silverberg, N. and Nuzzio, D.B., 1998. Simultaneous measurement of O_2, Mn, Fe, I^- and S(-II) in marine porewaters with a solid-state voltammetric micro-electrode, Limnol. Oceanogr. 43, 325-333.

Luther, III, G.W., Reimers, C.E., Nuzzio, D.B. and Lovalvo, D., 1999. In Situ deployment of voltammetric, potentiometric and amperometric microelectrodes from a ROV to determine O_2, Mn, Fe, S(-2) and pH in porewaters. Environ. Sci. Technol. 33, 4352-4356.

Luther III, G.W., Findlay, A.J., MacDonald, D.J., Owings, S.M., Hanson, T.E., Beinart, R.A. and Girguis, P.R., 2011. Thermodynamics and kinetics of sulfide oxidation by oxygen: a look at inorganically controlled reactions and biologically mediated processes in the environment. Frontiers in Microbiology, Vol. 2, Article 62, 1-9.

Millero, F.J., Plese, T., Fernandez, M., 1988. The dissociation of hydrogen sulfide in seawater. Limnol Oceanogr. 33: 269-274.

Morse, J.W, Millero, F.J., Cornwell, J.C., Rickard, D., 1987. The chemistry of the hydrogen sulfide and iron sulfide system in natural water. Earth-Science Reviews, 24:1-42.

Motelica-Heino, M., Naylor, C., Zhang, H. and Davison, W., 2003. Simultaneous release of metals and sulfide in lacustrine lacustrine sediment. Environ. Sci. Technol. 37(19):4374-4381.

Mousavi, M.F., Sarlack, N., 1997. Spectrophotometric determination of trace amounts of sulfide ion based on its catalytic reduction reaction with Methylene Blue in the presence of Te(IV). Anal. Lett. 30:1567-1578.

Naylor, C., Davison, W., Motelica-Heino, M., Van Den Berg, G.A. and Van Der Heijdt, A A., 2004. Simultaneous release of sulphide with Fe, Mn, Ni and Zn in marine harbour sediment measured using a combined metal/sulphide DGT probe. Sci. Tot. Environ. 328, 275-286.

Poulton, S.W., Krom, M.D. and Raiswell, R., 2004. A revised scheme for the reac-tivity of iron(oxyhydr)oxide minerals towards dissolved sulfide. Geochim. Cosmochim. Acta 68, 3703–3715.

Reija, B., Al-Soufi, W., Novo, M. and Tato, J.V., 2005. Specific interactions in the inclusion complexes of pyronines Y and B with β-cyclodextrin. J. Phys. Chem. B 109:1364-1370.

Revsbech, N.P., 2005. Analysis of microbial communities with electrochemical microsensors and microscale biosensor. In "Environmental Microbiology" (J.R. Leadbetter ed.), Methods in Enzymology Vol 397, pp.147-166. Academic Press, Oxford.

Robertson, D., Teasdale, P.R. and Welsh, D.T., 2008. A novel gel-based technique for the high resolution, two-dimensional determination of iron (II) and sulfide in sediment. Limnol. Oceanogr.: Methods 6:502–512.

Schröder, C.R., Polerecky, L. and Klimant, I., 2007. Time-resolved pH/pO_2 mapping with luminescent hybrid sensors. Anal. Chem. 79: 60-70.

Schippers A., Jørgensen B.B., 2002, Biogeochemistry of pyrite and iron sulfide oxidation in marine sediments, Geochim. Cosmochim. Acta 66(1): 85-92.

Shamsipur, M., Tashkhourian, J., Sharghi, H., 2005. Development of sulfide-selective optode membrane based on immunobilization of methylene blue on optically transparent triacetylcellulose film. Instrumentation Science and technology 33:703-714.

Stromberg, N. and Hulth, S., 2001. Ammonium selective fluorosensor based on the principles of coextraction. Anal. Chim. Acta. 443:215-225.

Stromberg, N. and Hulth, S., 2003. A fluorescence ratiometric detection scheme for ammonium ions based on the solvent sensitive dye MC 540. Sens. Actuators, B 90:308-318.

Swider, K.T. and Mackin, J.E. 1989. Transformations of sulfur compounds in marsh-flat sediments. Geochim. Cosmochim. Acta 53, 2311-2323.

Tang, D. and Santschi, P.H., 2000. Sensitive determination of dissolved sulfide in estuarine water by solid-phase extraction and high-performance liquid chromatography of methylene blue. J. Chromatogr. A 883:305-309.

Teasdale, P., Hayward, S. and Davison, W., 1999. In situ, high-resolution measurement of dissolved sulfide using diffusive gradients in thin films with computer-imaging densitometry. Anal. Chem. 71:2186-2191.

Wenzhöfer, F. and Glud, R.N., 2004. Small-scale spatial and temporal variability in coastal benthic O_2 dynamics: Effects of fauna activity. Limnol. Oceanogr. 49: 1471–1481.

Yücel, M., Luther, G.W. and Moore, W.S., 2010. Earthquake-induced turbidite deposition as a previously unrecog-nized sink for hydrogen sulfide in the Black Sea sediments. Mar. Chem. 121, 176–186.

Zhu, Q.Z., Aller, R.C. and Fan, Y., 2005. High-performance planar pH fluorosensor for two-dimensional pH measurements in marine sediment and water. Environ. Sci. Technol., 39: 8906-8911.

Zhu. Q.Z., Aller, R.C. and Fan, Y., 2006a. Two dimensional pH distributions and dynamics in bioturbated marine sediments. GeoChim. Cosmochim. Acta 70: 4933-4949.

Zhu, Q.Z., Aller, R.C. and Fan, Y., 2006b. A new ratiometric, planar fluorosensor for measuring high resolution, two-dimensional pCO_2 distributions in marine sediments. Mar. Chem. 101: 40-53.

Zhu, Q.Z. and Aller R.C., 2010. A rapid response, planar fluorosensor for measuring twodimensional pCO_2 distributions and dynamics in marine sediments. Limnol. Oceanogr.: Methods 8:326–336.

Zhu, Q.Z. and Aller R.C., 2012. Two-dimensional dissolved ferrous iron distributions in marine sediments as revealed by a novel planar optical sensor. Mar. Chem. 136-137:14-23.

Table 1. Effect of common gases on the sensor fluorescence intensity.

Foreign gas	Concentration	Relative error (%)
O_2	100%	0.3
N_2	100%	0.2
pCO_2	5	2.0
	10 matm	3.7
NH_3	0.15	1.8
	1.5	2.3
	15 mM	-4.4

Figure Captions

Fig. 1. Schematic drawing of the optical system for 2-D H_2S measurement in sediment. Inserted panel is a zoom into the cross section of sensor foil, layer 1, 2, and 3 are gas permeable silicone film, H_2S sensing film made of ethyl cellulose, and Mylar support sheet, respectively. The sensor foil can be introduced into sediment core along subcorer glass wall and 2-D fluorescence image is taken after the equilibration is set up between sensor and solutes in surrounding environment (~ 1 hour). A black plastic sheet is inserted vertically into the overlying water in the middle of the subcorer to ensure a featureless background within the water column.

Fig. 2. (A) Excitation spectra of free dissolved Pyronin Y in various sulfide solutions: (1) 0, (2) 0.5, (3) 1.0, and (4) 2.0 μM. (B) Excitation spectra of sensor foil in the presence of different concentration of H_2S: (1) 0, (2) 75, (3) 150, and (4) 300 μM.

Fig.3. The hypothesized reaction mechanism of Pyronin Y with hydrogen sulfide in the sensor membrane.

Fig. 4. Response characteristic and time of the planar H_2S fluorosensors. (A) The sensor M1 was exposed to anoxic H_2S solution, H_2S concentration was first increased and subsequently decreased. (B) The sensor M1 was exposed to an alternating H_2S concentration of 0 and 550 μM in buffer solution at room temperature. The sensor is reversible after the first cycle with t_{90} 60 s and R_{90} 30 s. (C) The response of sensor M2 to 0 and 12.5 μM H_2S .

Fig. 5. Response calibration of the planar H_2S fluorosensor. (A) M1 and (B) M2. The fluorescence intensity quenching extent (F_0/F) of M1 shows a good linearity against the concentration of H_2S, following Stern-Volmer equation. For the low level H_2S sensor M2, the fluorescence quenching (F_0-F) shows a good linearity to H_2S concentration.

Fig. 6. Two-dimensional H_2S distribution pattern (pseudocolored) in intertidal core and overlying water obtained from Flax Pond, Long Island, on Sept. 24, 2007. No distinct macrofauna and burrows are present. (A) A visible image of the sediment (green band). (B) Corresponding 2-dimensional H_2S distribution in sediment of panel (A). (C) The average vertical H_2S profile of panel (B) calculated from each horizontal pixel layer. Dashed line represents sediment surface.

Fig. 7. Spatial and temporal 2-D H_2S distribution patterns in a bioturbated salt marsh sediment obtained from Flax Pond (Long Island, NY). Upper green panels (A-F) are time series of visible images of intact sediment reworked by 5 pieces of *Nereis succine* (6 - 10 cm long), and the lower color panels are the corresponding 2-dimensional H_2S distribution patterns (A'-F'). Completely infilled relict burrows show light color in visible images and are marked with white arrows, inhabited burrows are pointed by black arrows. The lower and higher H_2S concentrations associated with inhabited and infilled burrows are clearly seen. Measurement time: (A, A') 1 hr; (B, B') 3 hrs; (C, C') 5 hrs; (D, D') 12 hrs, (E, E') 24 hrs; (F, F') 48 hrs.

Fig. 8. Significant heterogeneity of H_2S distribution in bioturbated sediment. (A) The average vertical H_2S profile calculated from Fig. 7D' (blue line, horizontal average) with minimum

(square) and maximum H_2S concentration (triangle) in the calculated horizontal layer. (B) The horizontal H_2S profile extracted from 2.5 cm depth in Fig 6D'.

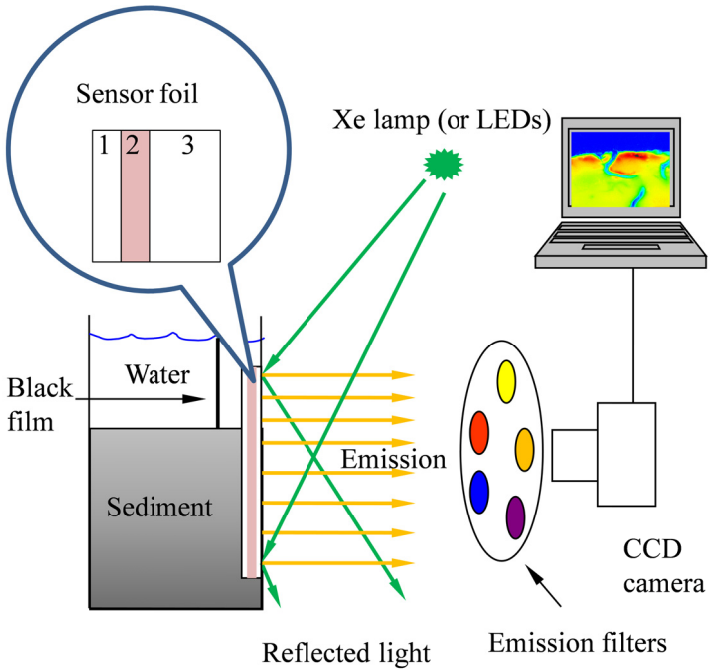
Sensor foil
1
2
3
Xe lamp (or LEDs)
Water
Black
film
Sediment
Emission
CCD
camera
Reflected light
Emission filters

Fig. 1

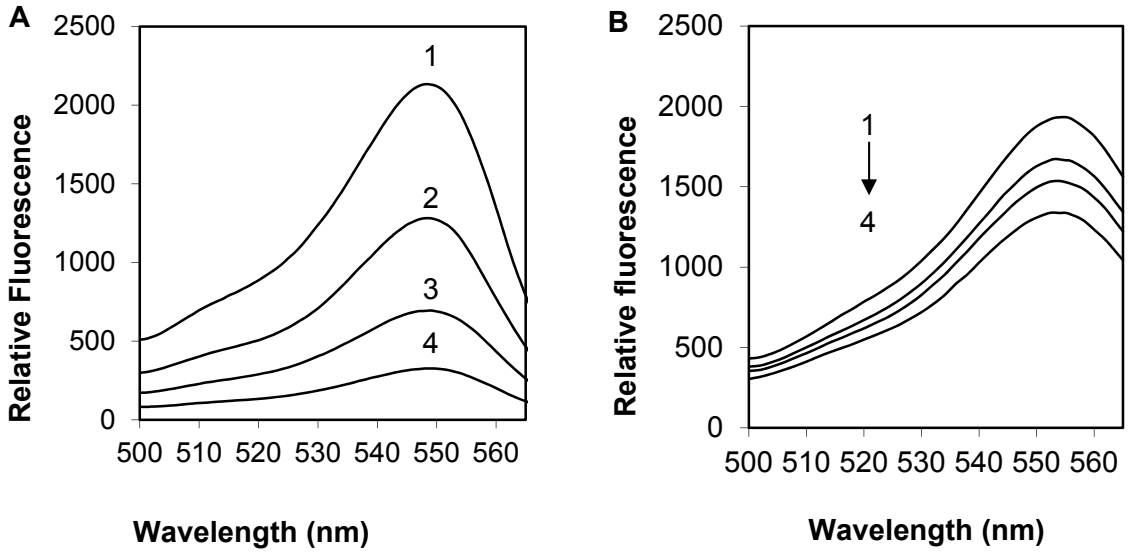
A
2500
2000
1500
1000
500
0
Relative Fluorescence
1
2
3
4
500 510 520 530 540 550 560
Wavelength (nm)
B
2500
2000
1500
1000
500
0
Relative fluorescence
1
4
500 510 520 530 540 550 560
Wavelength (nm)

Fig. 2.

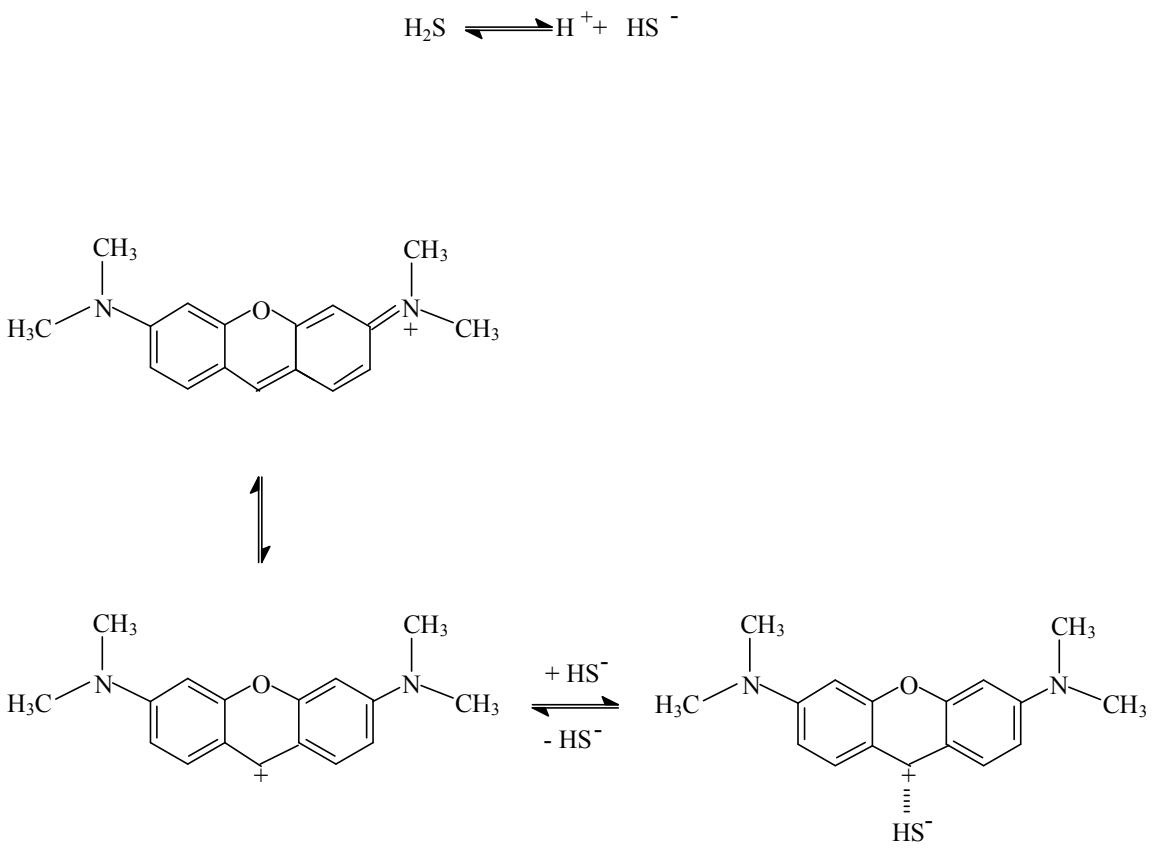
H2S
H+ + HS-
CH3
H3C
N
O
N
CH3
+
+ HS-
- HS-
HS-
Strong fluorescence
Non-fluorescence

Fig. 3.

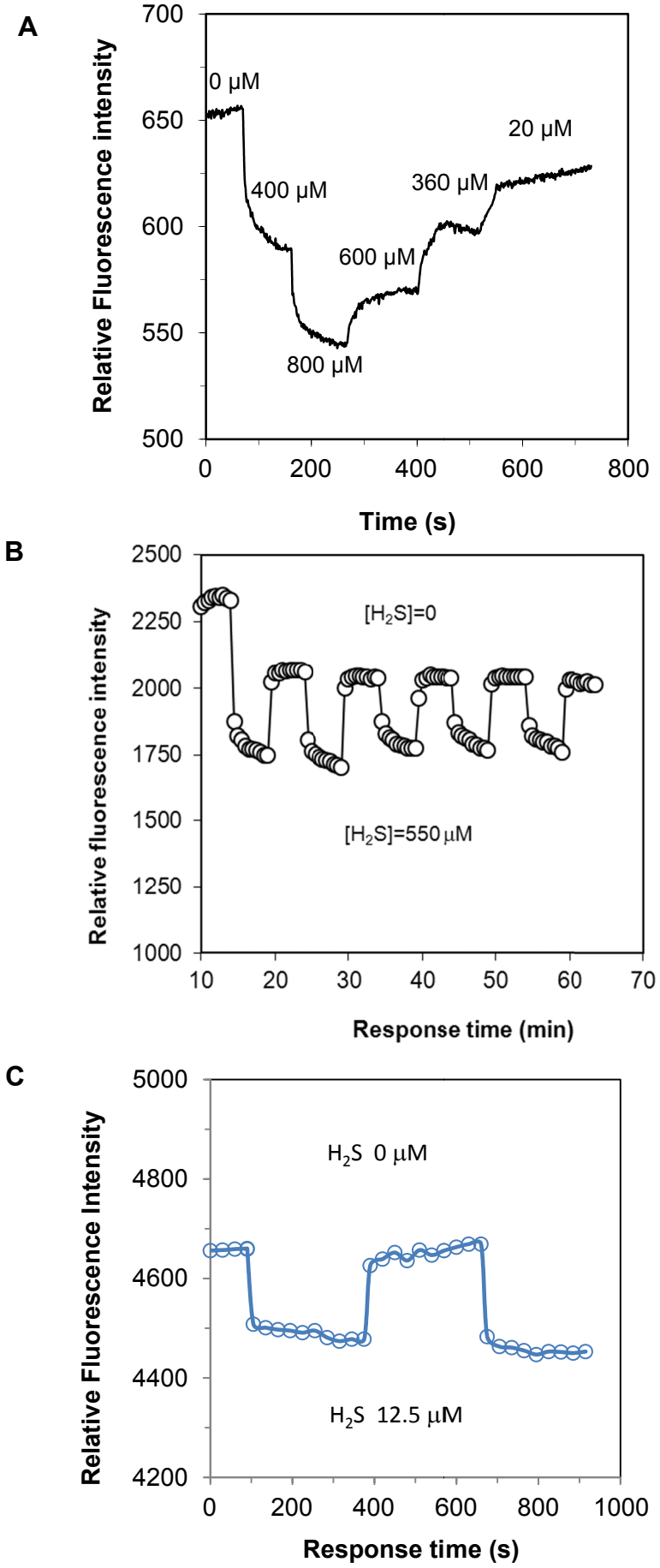
A
Relative Fluorescence intensity
700
650
600
550
500
0 μM
400 μM
800 μM
600 μM
360 μM
20 μM
0
200
400
600
800
Time (s)
B
Relative fluorescence intensity
2500
2250
2000
1750
1500
1250
1000
[H2S]=0
[H2S]=550 μM
10
20
30
40
50
60
70
Response time (min)
C
Relative Fluorescence Intensity
5000
4800
4600
4400
4200
H2S 0 μM
H2S 12.5 μM
0
200
400
600
800
1000
Response time (s)

Fig. 4.

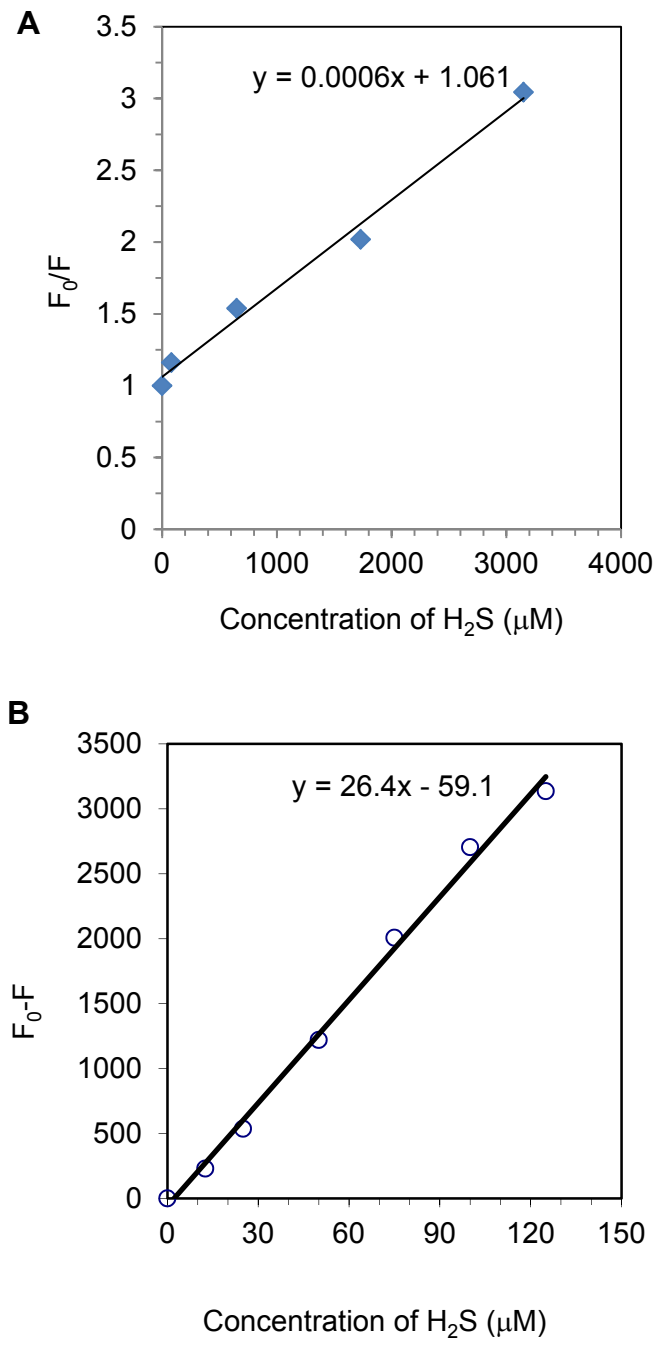
A
y = 0.0006x + 1.061
F0/F
3.5
3
2.5
2
1.5
1
0.5
0
0
1000
2000
3000
4000
Concentration of H2S (μM)
B
y = 26.4x - 59.1
F0-F
3500
3000
2500
2000
1500
1000
500
0
0
30
60
90
120
150
Concentration of H2S (μM)

Fig. 5.

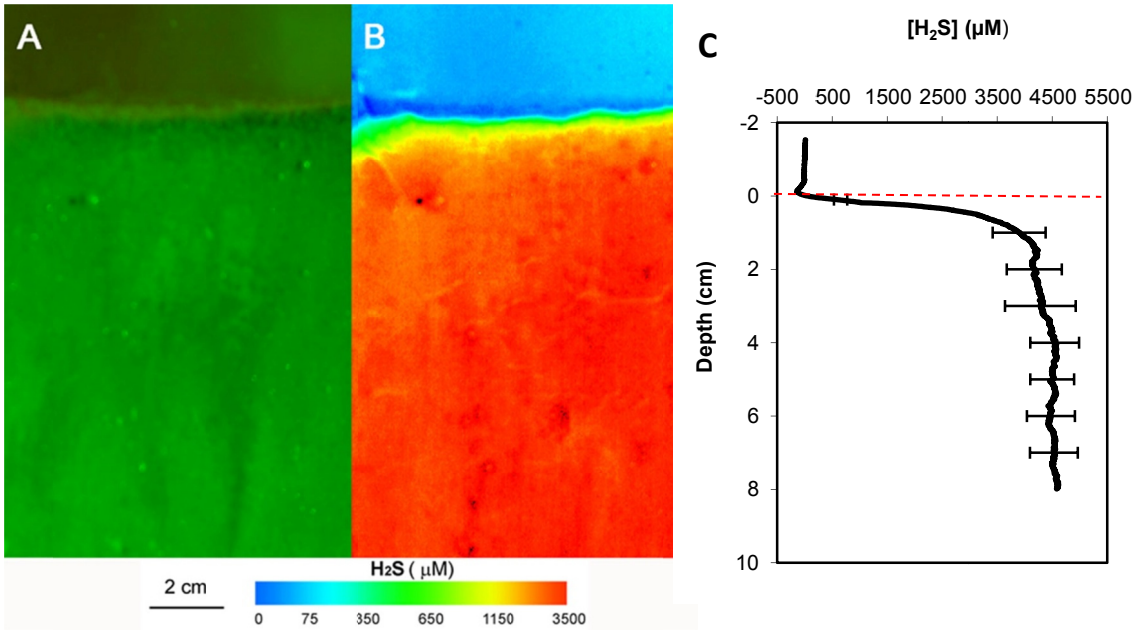
A
B
C
[H2S] (μM)
-500 500 1500 2500 3500 4500 5500
-2
0
2
4
6
8
10
Depth (cm)
2 cm
H2S (μM)
0 75 350 650 1150 3500

Fig. 6.

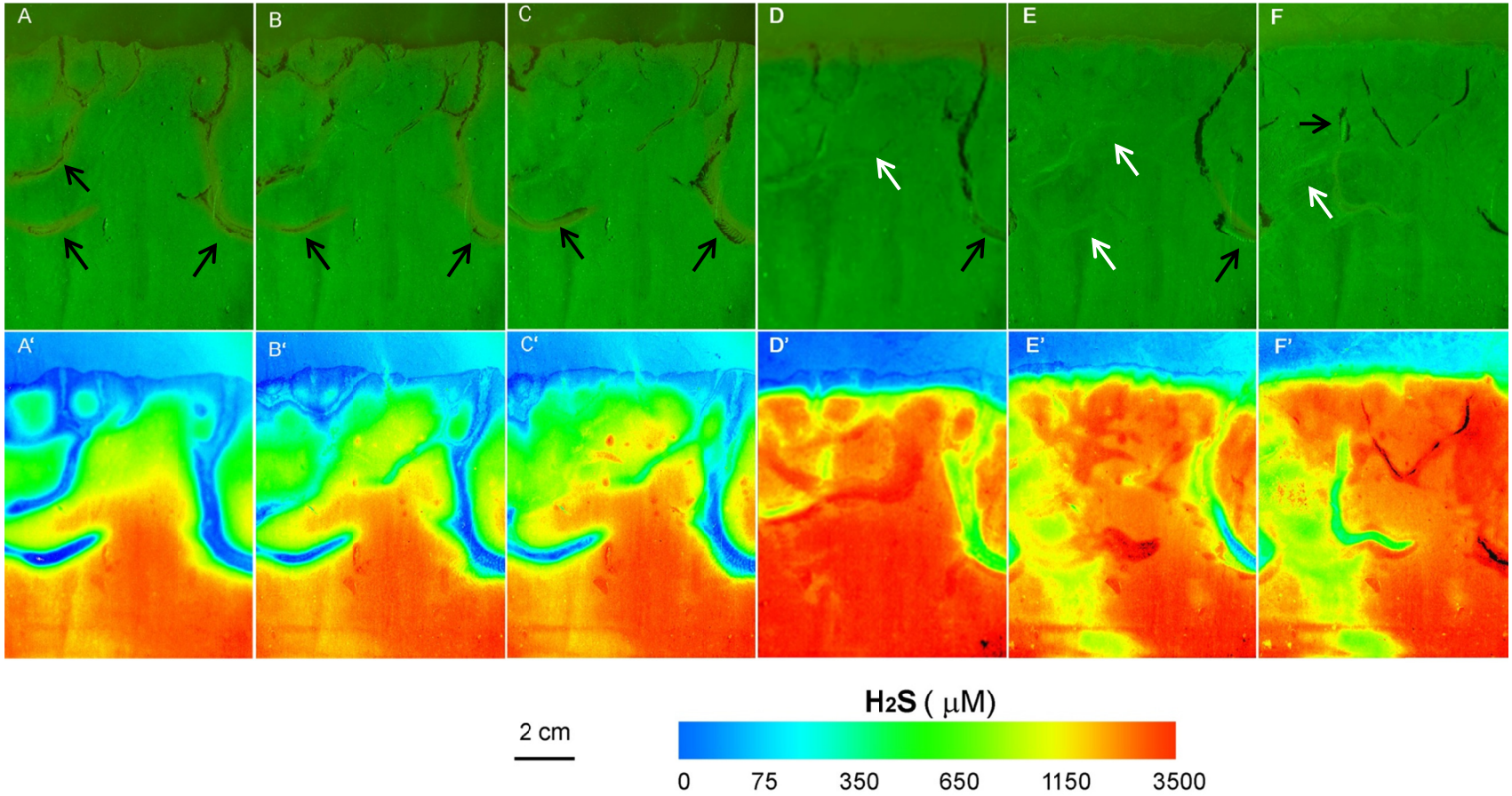

Fig. 7.

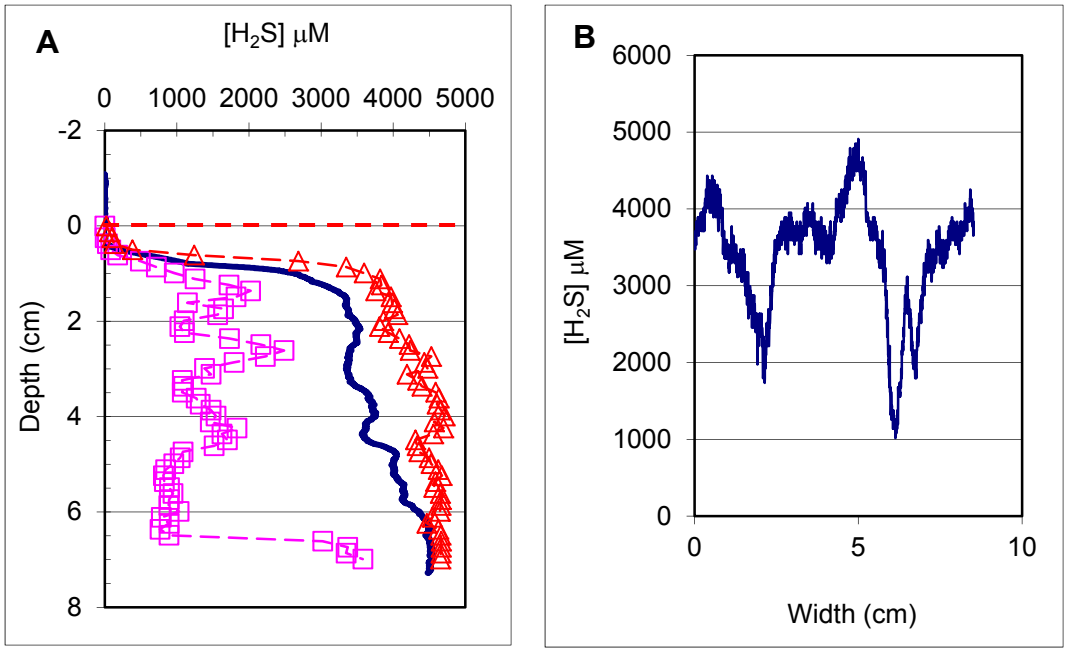
A
[H2S] µM
0
1000
2000
3000
4000
5000
-2
0
2
4
6
8
Depth (cm)
B
6000
5000
4000
3000
2000
1000
0
[H2S] µM
0
5
10
Width (cm)

Fig. 8.